Supplemental Material for Magnetic field and temperature sensing with atomic-scale spin defects in silicon carbide

H. Kraus[1], V. A. Soltamov[2], F. Fuchs[1], D. Simin[1], A. Sperlich[1],
P. G. Baranov[2], G. V. Astakhov[1,*] and V. Dyakonov[1,3†]
[1]*Experimental Physics VI, Julius-Maximilian University of Würzburg, 97074 Würzburg, Germany*
[2]*Ioffe Physical-Technical Institute, 194021 St. Petersburg, Russia*
[3]*Bavarian Center for Applied Energy Research (ZAE Bayern), 97074 Würzburg, Germany*

I. CALCULATION OF THE ODMR SPECTRA

We consider a spin defect with the symmetry axis along the z-axis. The external magnetic field B lies in the xz-plane and its orientation is given by the polar angle θ, such that $B_z = B\cos\theta$ and $B_x = B\sin\theta$. The spin Hamiltonian for the $S = 3/2$ system is written in the form

$$\mathcal{H} = g_e\mu_B B(S_z\cos\theta + S_x\sin\theta) + D(S_z^2 - \frac{5}{4}\mathcal{I})\,. \tag{S1}$$

Here, $\mathcal{I}$ is the unit matrix, S_z and S_x denote the spin matrices

$$S_z = \begin{bmatrix} \frac{3}{2} & 0 & 0 & 0 \\ 0 & \frac{1}{2} & 0 & 0 \\ 0 & 0 & -\frac{1}{2} & 0 \\ 0 & 0 & 0 & -\frac{3}{2} \end{bmatrix}, \quad S_x = \begin{bmatrix} 0 & \frac{\sqrt{3}}{2} & 0 & 0 \\ \frac{\sqrt{3}}{2} & 0 & 1 & 0 \\ 0 & 1 & 0 & \frac{\sqrt{3}}{2} \\ 0 & 0 & \frac{\sqrt{3}}{2} & 0 \end{bmatrix}. \tag{S2}$$

The numerical solution of the Hamiltonian (S1) gives the eigenstates E_k and the eigenfunctions in the basis

$$\psi_k = \begin{bmatrix} a_{3/2} \\ a_{1/2} \\ a_{-1/2} \\ a_{-3/2} \end{bmatrix}. \tag{S3}$$

It is instructive to consider analytically weak magnetic fields $g_e\mu_B B \ll 2D$, which is the most relevant for magnetic field sensing. In this case, the $m_s = \pm 3/2$ and $m_s = \pm 1/2$ states can be considered separately. For the $m_s = \pm 3/2$ states the Hamiltonian (S1) is simplified to the form

$$\mathcal{H} = \frac{3}{2}g_e\mu_B B \begin{bmatrix} \cos\theta & 0 \\ 0 & -\cos\theta \end{bmatrix} + D \tag{S4}$$

and the solution is $E_{1,4} = D \pm \frac{3}{2}g_e\mu_B B\cos\theta$ with the eigenfunctions

$$\psi_1 = \begin{bmatrix} 1 \\ 0 \\ 0 \\ 0 \end{bmatrix}, \quad \psi_4 = \begin{bmatrix} 0 \\ 0 \\ 0 \\ 1 \end{bmatrix}. \tag{S5}$$

For the $m_s = \pm 1/2$ states the Hamiltonian (S1) is simplified to the form

$$\mathcal{H} = \frac{1}{2}g_e\mu_B B \begin{bmatrix} \cos\theta & 2\sin\theta \\ 2\sin\theta & -\cos\theta \end{bmatrix} - D \tag{S6}$$

*E-mail: astakhov@physik.uni-wuerzburg.de
†E-mail: dyakonov@physik.uni-wuerzburg.de

and the solution is $E_{2,3} = -D \pm \frac{1}{2} g_e \mu_B B \sqrt{1 + 3\sin^2\theta}$ with the eigenfunctions

$$\psi_2 = \begin{bmatrix} 0 \\ \sqrt{\frac{1}{2} + \frac{\cos\theta}{2\sqrt{1+3\sin^2\theta}}} \\ \sqrt{\frac{1}{2} - \frac{\cos\theta}{2\sqrt{1+3\sin^2\theta}}} \\ 0 \end{bmatrix}, \quad \psi_3 = \begin{bmatrix} 0 \\ \sqrt{\frac{1}{2} - \frac{\cos\theta}{2\sqrt{1+3\sin^2\theta}}} \\ \sqrt{\frac{1}{2} + \frac{\cos\theta}{2\sqrt{1+3\sin^2\theta}}} \\ 0 \end{bmatrix}. \tag{S7}$$

One can see from Eq. (S7) that the $m_s = \pm 1/2$ states are mixed in the transverse component of the magnetic field. This results in four possible RF-driven transitions (see Fig. 2 of the main text). The exclusion, when only two RF-driven transitions are observed, is for three specific polar angles $\theta = 0°$, $\theta = 90°$ and $\theta = \arccos(1/\sqrt{3}) \approx 54.7°$.

We have calculated the relative probabilities of these transitions between the j-th and k-th spin sublevels using

$$W_{jk} \sim \left| B_{1y} \langle j | S_y | k \rangle \right|^2 . \tag{S8}$$

Here, the RF driving field B_{1y} is applied along the y-axis, i.e., perpendicular to the defect symmetry axis and the magnetic field B. In order to account for the optical spin pumping, we assume the same optically induced depletion of the $m_s = +1/2$ and $m_s = -1/2$ states. This means that there is no RF-induced transitions between these states, which is taken into account by setting to zero the corresponding components of the spin matrix in (S8):

$$S_y = \begin{bmatrix} 0 & -i\frac{\sqrt{3}}{2} & 0 & 0 \\ i\frac{\sqrt{3}}{2} & 0 & 0 & 0 \\ 0 & 0 & 0 & -i\frac{\sqrt{3}}{2} \\ 0 & 0 & i\frac{\sqrt{3}}{2} & 0 \end{bmatrix}. \tag{S9}$$

The results of these calculations are color-coded in Fig. 2(a) of the main text.

It is worth to note that in our experiments the RF field is not exactly parallel to the y-axis. To calculate the RF-induced transitions for arbitrage orientation of B_1 we use Eq. (2) in the main text and from the best fit of the ODMR line amplitudes in Fig. 4(b) we find the angle between B_1 and the c-axis of SiC is 65°.

II. LASER EFFECT ON THE ODMR SPECTRA

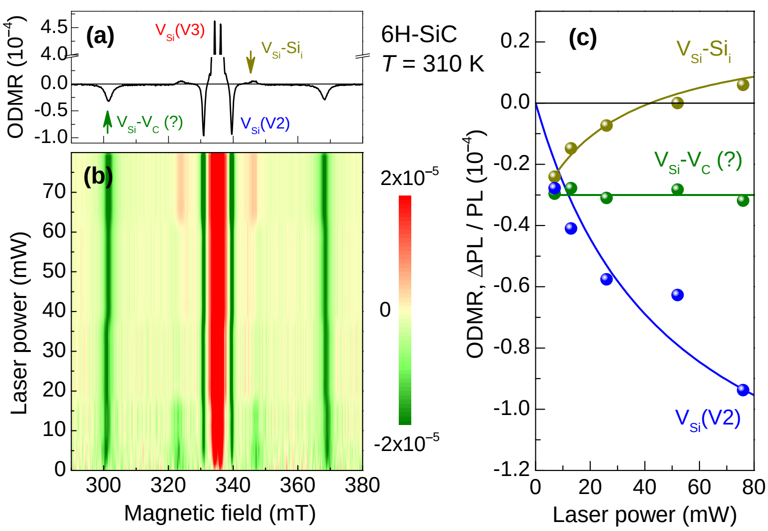

FIG. S1: (a) An ODMR spectrum of 6H-SiC obtained at a laser power $P = 76$ mW. (b) Laser power dependence of the ODMR spectra. (c) The ODMR contrast of different defects as a function of laser power.

We have measured ODMR spectra as a function of laser power P to determine the laser-induced heating in our SiC samples. We monitor the temperature variation with P using the V_{Si}-V_C defect as an internal thermometer

[Fig. S1(b)]. At $P = 76$ mW the V_{Si}-V_C ZFS is reduced by 2.3 MHz [Fig. S1(a)], which corresponds to a temperature increase by $\Delta T = 2.1$ K.

Remarkably, the ODMR contrast ΔPL/PL as a function of P reveals qualitatively different behavior for different defects [Fig. S1(c)]. For the V_{Si}(V2) defect ΔPL/PL being proportional to the optically-induced spin polarization is well described by

$$\frac{\Delta \mathrm{PL}}{\mathrm{PL}} = \frac{\alpha_0}{1 + P_0/P}\,, \tag{S10}$$

where $\alpha_0 = -1.5 \times 10^{-4}$ is the ODMR contrast in saturation and $P_0 = 50$ mW is a characteristic pump power (the laser is focused onto a spot of about several hundreds micrometers in diameter).

The ODMR contrast for the V_{Si}-V_C defect is constant $\alpha_0 = -0.3 \times 10^{-4}$ down to the laser power when the PL is still detectable, i.e., $P_0 \ll 7$ mW, indicating a very efficient optical spin pumping mechanism.

For the V_{Si}-Si_i Frenkel pair the ODMR contrast changes its sign with increasing P [Figs. S1(b) und (c)], which is quite unusual. We expect that the position of the interstitial Si atom within the Frenkel pair is very sensitive to the local strain and/or electric field, which in turn can be induced by photo-(di)charging of the defects nearby.

[1] Riedel, D. *et al.* Resonant Addressing and Manipulation of Silicon Vacancy Qubits in Silicon Carbide. *Physical Review Letters* **109**, 226402 (2012).

[2] von Bardeleben, H., Cantin, J., Henry, L. & Barthe, M. Vacancy defects in p-type 6H-SiC created by low-energy electron irradiation. *Physical Review B* **62**, 10841–10846 (2000).